

Prediction of BLEVE loads on structures using machine learning and CFD

Qilin Li^a, Yang Wang^b, Ling Li^{a,*}, Hong Hao^b, Ruhua Wang^b, Jingde Li^b

^a Discipline of Computing, School of Electrical Engineering, Computing and Mathematical Sciences, Curtin University, Australia

^b Centre for Infrastructural Monitoring and Protection, School of Civil and Mechanical Engineering, Curtin University, Australia

ARTICLE INFO

Keywords:

Gas explosion
BLEVE
Transformer
Machine learning
Blast wave
Interaction with structures
CFD
Neural networks

ABSTRACT

Boiling Liquid Expanding Vapour Explosions (BLEVEs) are driven by complex fluid dynamics with expanded vapour and flashed liquid. They may generate strong shock waves that lead to catastrophic consequences to personnel and structures in the vicinity. Despite the great interest in safety management and intensive research efforts, reliable and efficient prediction of BLEVE loads on structures is still challenging in practice. Computational Fluid Dynamics (CFD), based on complex physics formulas, can provide more accurate predictions of BLEVE loads than the traditional empirical and TNT-equivalency approaches, but suffers from high computational costs. Data-driven machine learning models offer efficient surrogates but conventional models, including commonly used multi-layer perceptron (MLP), are suboptimal especially for explosions of complex geometry and in complex environment. In this study, a novel machine learning approach, based on the state-of-the-art Transformer neural networks, is developed for BLEVE loads prediction on an idealised structure in the vicinity of BLEVE. Through extensive experiments and rigorous evaluation, it is shown that Transformer can effectively model the structure-wave interaction, yielding accurate pressure and impulse predictions with less than 14% relative errors, which outperforms widely used MLP (20% error) significantly. The developed Transformer model is applied to predict critical parameters of BLEVE loads, including arrive time, rise time and duration. The results demonstrate that Transformer can produce an accurate pressure-time history, yielding a comprehensive characterisation of BLEVE loads on structures.

1. Introduction

Boiling Liquid Expanding Vapour Explosion (BLEVE) (Birk and Cunningham, 1994) is one of the main types of gas explosions that occur frequently in recent decades, often resulting in catastrophic consequences (Wang et al., 2022a; Török et al., 2011; Abbasi and Abbasi, 2007). BLEVE occurs when the temperature of the liquid inside the tank exceeds its atmospheric boiling point and the pressurised tank ruptures suddenly (Paltrinieri et al., 2009). The liquid vaporises and the vapour expands extremely rapidly, releasing a large amount of energy with threatening blast waves (Mitu et al., 2016; CCPS, 2011). Moreover, BLEVE can trigger the domino effect and lead to more concerning hazards, such as fire and multiple explosions (Hemmatian et al., 2015; Spoelstra et al., 2015).

Studies of BLEVE in open space have been conducted (Li et al., 2021a; Wang et al., 2022b), in which the blast wave propagation and the corresponding overpressures can be predicted accurately. However, for the effective design of structures against BLEVE loads, prediction of

BLEVE blast waves acting on the structures is needed. Prediction of BLEVE loads on structures is more complex than predictions of blast wave propagations in open space, since the interaction between blast wave and structure needs to be considered and it is affected by many factors such as the blast wave velocity, incident angle, structural geometry, dimension, and stiffness, as well as the surrounding environments. In this paper, as an extension of the previous studies on predicting the open space BLEVE pressures (Li et al., 2021a; Wang et al., 2022b), the interaction of BLEVE wave with structures is modelled for BLEVE loads prediction. The structure is modelled as a rigid body, which is a common assumption in most studies of modelling the interaction between explosion wave and structure (Shi et al., 2007), i.e., the influence of structural deformation on blast wave-structure interaction is ignored. A standalone cuboid structure is placed near the BLEVE source, and we are interested to predict the blast loads, such as pressure and impulse, on different faces of the structure.

There are two commonly used approaches for the prediction of BLEVE loads in practice: the energy equivalence method based on TNT

* Corresponding author.

E-mail addresses: qilin.li@curtin.edu.au (Q. Li), yang.wang17@postgrad.curtin.edu.au (Y. Wang), l.li@curtin.edu.au (L. Li), hong.hao@curtin.edu.au (H. Hao), ruhua.wang@curtin.edu.au (R. Wang), jingde.li@curtin.edu.au (J. Li).

blast charts and the numerical simulation based on Computational Fluid Dynamics (CFD). Energy equivalence methods are derived from various thermodynamics assumptions. Hemmatian et al. (2017) provided a detailed review of empirical methods for modelling BLEVE mechanical energy for the prediction of BLEVE waves. These energy equivalence methods are based on some assumptions which are not straightforward to make. Furthermore, the pressure wave profile predicted by TNT-equivalency method could be very different from those induced by BLEVE in terms of the rise time, amplitude and duration. Therefore, energy equivalence methods may not yield good predictions of BLEVE pressures as demonstrated in Hao et al. (2016) and Wang et al. (2022b).

On the other hand, CFD can accurately model blast wave propagation in a complex environment based on detailed numerical simulations. Several preliminary studies have shown that carefully validated CFD model can yield reliable BLEVE overpressure predictions (Hansen and Kjellander, 2016; Hutama, 2017; Li et al., 2018). Further studies have also been conducted recently to model the BLEVE energy distribution more accurately, by considering the fact that the BLEVE source contains two high-pressure regions. Since the BLEVE tank is a pressurised vessel that contains both vapour and liquid phases, two high-pressure regions need to be modelled. However, only one high-pressure region can be defined in the current CFD models, such as FLACS. To address this limitation, Li and Hao (2020) proposed the liquid correction method and the shock tube method, introducing a pseudo-source to model the second high-pressure region. Since the shock tube method requires more preliminary assumptions while the liquid correction method was proved to be accurate and easier to use, the latter method has been used in subsequent studies to simulate BLEVE wave propagations in open space and interaction with obstacles, i.e., modelling the interaction of blast wave with one or a group of cylindrical obstacles and estimate the reflected pressures on the front and rear surface of cylinders (Li and Hao, 2021).

To the best of our knowledge, there are limited studies of BLEVE occurring in the obstructed environment and no experimental data is publicly available either. Therefore, predictions of BLEVE wave propagation and interaction with obstacles in complex environments depend on using verified CFD models. Despite the high accuracy of CFD simulations of BLEVE pressure wave propagations, the major drawback is the efficiency and cost. A CFD model simulation of a BLEVE event and the corresponding wave propagation and interaction with surrounding structures can take hours or even days. It also requires profound CFD modelling knowledge as well as the relevant facilities and specific software codes that are not readily available in most consulting firms. These make the detailed CFD model simulations difficult or even not practical in practice for prediction of BLEVE loading on structures for engineering design application.

To alleviate the computational burden for efficient and reliable BLEVE loading predictions, recent studies attempted to use machine learning approaches for BLEVE modelling. These approaches are data-driven, i.e., training data are needed to “teach” the model how to map from input variables to the desired target output. Despite the computationally intensive training phase, the model can make fast predictions once trained. The fully connected feed-forward artificial neural network, also known as Multi-Layer Perceptron (MLP), has been widely used for BLEVE prediction. For example, Hemmatian et al. (2020) estimated the butane and propane BLEVE mechanical energy using MLP, in which training data came from empirical models based on real gas behaviour and adiabatic irreversible expansion assumption. Li et al. (2021a) showed that an accurate and efficient MLP model could be constructed based on simulated training data from a validated CFD model. Wang et al. (2022b) continued the study to derive BLEVE pressure prediction equations and charts in open space using the surrogate MLP model due to its efficiency. These studies demonstrated that using machine learning approaches in conjunction with CFD for BLEVE modelling is promising. Existing investigations, however, are limited to exploring the machine learning approaches in predicting the BLEVE pressures in open space,

and there is no justification or evaluation on the choice of MLP models compared to other machine learning models. Recently, Li et al. (2023) conducted a comparative study on the most effective machine learning model for blast load prediction and reported that Transformer neural network (Vaswani et al., 2017) can achieve the best accuracy for the BLEVE pressure prediction in the open space, outperforming widely used MLP and other competitors. It was also discussed that the superior performance of Transformer is due to its larger model capacity, and therefore it was believed that the advantage of Transformer would be even more prominent when used for more complicated cases, e.g., prediction of BLEVE loads with obstacles.

Since the primary purpose of modelling and predicting the BLEVE wave propagation is to evaluate its risk and to design appropriate measures for people and structure protection, it is important to predict BLEVE load acting on the structure, i.e., reflected pressures and impulses, besides predicting blast waves in open space. This study hence extends the authors' previous work in predicting blast waves in the open space to predict the reflected BLEVE pressure and impulse on a rectangular rigid structure at different standoff distances from the BLEVE source. First, a CFD model is constructed and validated using open-space BLEVE experimental data. The established CFD model is then used to simulate BLEVE wave propagation and interaction with a rigid structure in various settings, such as structure dimensions, standoff distances, and facing angles, etc. The simulated parameters of reflected pressure and impulse are used to train a surrogate machine learning model, for efficient predictions of BLEVE loading. It is formulated as a regression problem, in which the settings of the BLEVE source and structure serve as the input and the critical blast parameters of interest act as the output.

Following the comparative study (Li et al., 2023), the state-of-the-art Transformer model is used, which outperforms MLP with clear margins on all BLEVE loads related parameters, e.g., for peak pressure prediction, Transformer achieves a relative error of 13.4% and R^2 0.933 compared to 18.0% and 0.858 by MLP. A comprehensive analysis of the Transformer prediction is also performed to study if the model is biased to certain BLEVE conditions, such as the loading scale and sensor location. The developed Transformer model is then applied to predict all critical parameters related to BLEVE loads, including arrive time, rise time, and duration of blast waves. The results show that the pressure-time profile predicted by Transformer is well aligned with the one from FLACS simulation, providing a detailed characterisation of the BLEVE loads on structures.

The rest of the paper is organised as follows: numeric modelling and data simulation are introduced in Section 2. The methodology and implementation of the Transformer model are presented in Section 3. The experimental results are shown in Section 4. The conclusion is drawn in Section 5.

2. Numerical modelling

2.1. Validation of FLACS simulation

The most commonly used commercial CFD software for numerical analysis of gas explosions is FLACS, which can solve the Favre-averaged transport equations in 3D for mass, momentum, enthalpy, and turbulent kinetic energy, etc. The Reynolds-averaged Navier-Stokes equations are applied for ideal gas law and the standard k- ϵ model for turbulence modelling (Lauder and Spalding, 1983). The Euler equations, flux-corrected transport scheme and a second-order flux correction are employed to model the detonation of condensed explosive and blast wave propagations using the FLACS-Blast module. Cell-centred grids are used to solve scalar variables (i.e., pressure, temperature and density), while staggered grids are used to solve velocity components (Gexcon, 2017).

18 recorded pressure time histories from BLEVE experiments containing both butane and propane conducted by Johnson and Pritchard (1990), Birk and VanderSteen (2006) and Birk et al. (2007), are used to

validate the FLACS simulation. The details of the BLEVE experiments are illustrated in Table 1. These represent the most available BLEVE test data in open literature owing to the general lack of BLEVE experimental studies. In the tests, the pressure sensors are generally arranged in a line along the BLEVE centre (i.e., x-direction), as shown in Fig. 1. To speed up computation in FLACS, a “SYMMETRY” boundary is applied on the x-z plane so that only one-half of the domain needs to be simulated, while a “PLANE_WAVE” boundary is used on x-y and y-z planes to minimise the boundary reflection. The grid size is a sensitive parameter in terms of the simulation efficiency and accuracy, which needs to be carefully analysed. A coarse grid size may yield inaccurate results, while a fine grid size leads to high computation costs. It is essential to find a suitable grid size to obtain the simulation results efficiently and accurately (Gebreslassie et al., 2012). The grid sensitivity analysis of FLACS for BLEVE simulations is performed by Li and Hao (2020) and Li et al. (2021a), using open-space BLEVE experimental data. It was found that the 0.2 m grid achieves the best trade-off between accuracy and efficiency. The grid sensitivity analysis for modelling BLEVE pressure wave interaction with obstacles is conducted in this study. Fig. 2 presents the convergence curve of the overpressure against the ratio of standoff distance to grid size. Note that this ratio is considered (as opposed to grid size only) because the error is accumulated during the computation of wave propagation. The overpressure on the centre of obstacle frontal face with a standoff distance of 20 m is monitored using grid sizes from 0.5 m to 0.1 m. As shown in Fig. 2, reducing grid size from 0.5 to 0.1 m, the overpressure is more than doubled, which highlights the importance of grid sensitivity study. The fitted curve indicates that the overpressure converges to around 20 kPa and only grid sizes 0.1 m, 0.15 m and 0.2 m produce predictions close to 20 kPa (with a relative difference of less than 20%). While grid sizes 0.1 m and 0.15 m may produce slightly better results, it comes with huge computational costs, e.g., it takes around 30 h, 12 h, and 6 h per case (10-core 3.3 GHz CPU) when using grid sizes 0.1, 0.15, and 0.2 m, respectively, which means using 0.2 m grid saves around 50% and 80% computation time compared to 0.15 and 0.1 m grids. Considering the large amount of simulation cases needed for the training of machine learning models, 0.2 m is used as the uniform grid size for all three directions in the region that contains the BLEVE source and the structure. The grid size for other regions is stretched progressively with a factor of 1.1 to further speed up the CFD simulation. In addition, BLEVE cases are examined to determine if the liquid status is either “superheated” or “non-superheated”, and the liquid correction method (Li and Hao, 2021) is applied to calculate the BLEVE rupture pressure for “superheated” cases.

The accuracy of the pressure-time history simulated by FLACS is illustrated in Fig. 3 which compares a typical experiment result of Birk's No. 02–01 at 20 m and the corresponding simulation result as an example. It shows that the FLACS simulation results can predict the first peak overpressure well, while the third peak overpressure is not well modelled due to more oscillations generated by FLACS. The third peak overpressure is usually small (i.e., less than 3 kPa) since it is created by the expansion of liquid flashing, which is generally not a safety concern to the structure. The 18 peak overpressures, which is the main interest in this study, from the tests and numerical simulations are compared. The comparison results are shown by the scatter plot in Fig. 4. The FLACS

simulation data X_p agree well with the experimental data X_o , where most of them are within 30% relative error. The simulation is further validated using the geometric mean bias (MG), geometric mean-variance (VG) and a factor of two (FAC2), which are defined as follows:

$$MG = \exp \left[\ln \left(\frac{X_p}{X_o} \right) \right] \quad (1)$$

$$VG = \exp \left[\ln \left(\frac{X_p}{X_o} \right)^2 \right] \quad (2)$$

$$FAC2 = \text{the fraction of data where } 0.5 \leq \frac{X_p}{X_o} \leq 2.0 \quad (3)$$

According to the FLACS operating guideline, the simulation performance is categorised as follows (Gexcon, 2017):

- Excellent: if $0.7 < MG < 1.3$, $VG < 1.6$, and $FAC2 > 75\%$.
- Acceptable: if $0.5 < MG < 2.0$, $1.6 < VG < 3.3\%$, and $50\% < FAC2 < 70\%$.
- Poor: if the measured variable is beyond the “acceptable” range.

The MG value represents the systematic results, while VG represents the scatter of the simulation results around the experimental data. By plotting the MG versus VG, we obtain the parabola plot in Fig. 5, which shows that most of the simulations are within the “Excellent” performance region, and all simulations are “Acceptable”. Meanwhile, all the simulations have a reasonable X_p/X_o value (i.e., between 0.5 and 2), indicating that the FLACS model can accurately model BLEVE for both butane and propane.

It should be noted that the above validations are based on experimental data in open space only because no BLEVE test data in congested environment is available in open literature. In other words, no test data is available to validate the FLACS simulation of BLEVE pressure wave interaction with structures. Although the simulation results of BLEVE cannot be directly compared with experiments in obstructed environments, the accuracy of FLACS software in predicting wave interactions with structures has been extensively verified. For example, Middha et al. (2007) performed a hydrogen explosion in a confined tube with obstacles, and the predicted results agree well with experimental data, proving FLACS can accurately predict pressure wave interactions with obstacles in such complex environments. Li and Hao (2019) predicted the gas explosion overpressure between two tanks in a site with a group of tanks. The numerical simulation results demonstrated that the modelling yielded reasonable accuracy in overpressure prediction on obstacles' walls as compared to experimental results. (Hutama, 2017) and (Li et al. 2021b) simulated BLEVEs in a tunnel and illustrated that the reflected blast waves could be predicted accurately using FLACS. Therefore, it can be concluded that FLACS can well simulate the blast wave interaction with structures in an obstructed environment.

2.2. Generation of training data for machine learning models

With the validated CFD model in FLACS, we generate a large dataset of BLEVE pressure waves by varying various parameters related to the BLEVE source, structure dimension and standoff distance from the

Table 1

BLEVE experiments used for model validation (Johnson and Pritchard, 1990; Birk and VanderSteen, 2006; Birk et al., 2007).

Test No.	Fluid	P_{rup} (MPa)	V (m^3)	D (m)	T_l (K)	LFL (%)	Liquid Status at failure	Distance (m)	P_{tot} (MPa)
02–01 (Birk)	Propane	1.80	2.00	1	330	51	Superheated	10/20/30/40	2.84
02–02 (Birk)	Propane	1.56	2.00	1	320	52	Superheated	10/20/30/40	2.46
02–03 (Birk)	Propane	1.81	2.00	1	325	53	Non-superheated	10/20/30/40	1.81
BG–2 (Johnson)	Butane	1.52	5.66	1.2	374	39	Superheated	25/50/100	2.57
BG–3 (Johnson)	Butane	7.5	5.66	1.2	323	68	Non-superheated	25/50/100	0.75

Note: failure pressure (P_{rup}), BLEVE tank volume (V), diameter of BLEVE tank (D), liquid failure temperature (T_l), liquid fill level (LFL) and total failure pressure in CFD model (P_{tot})

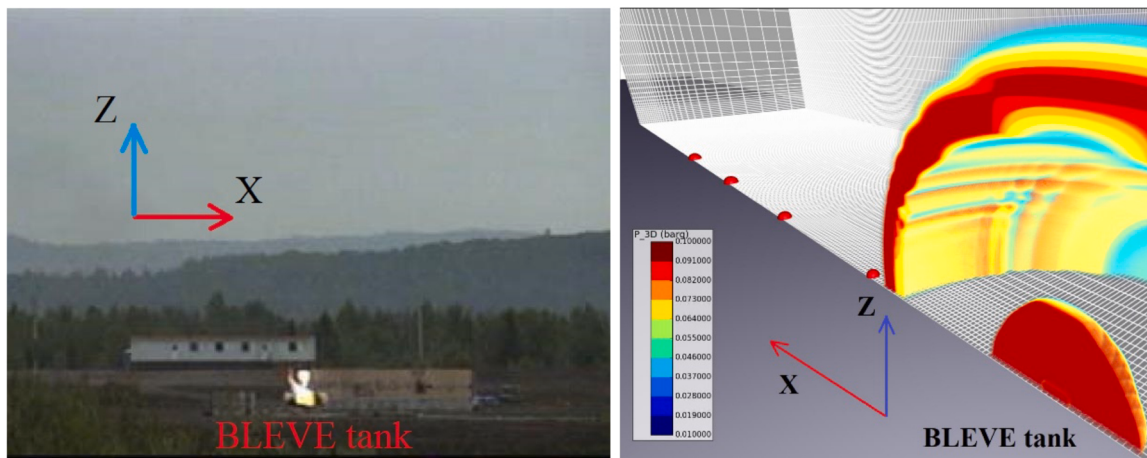


Fig. 1. Birk's BLEVE test No. 02–01 (left) (Birk et al., 2007) and CFD model (right) (Li et al., 2021a).

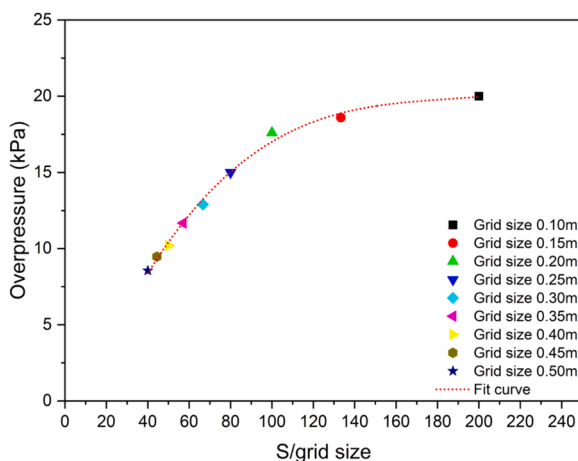


Fig. 2. Grid sensitivity study.

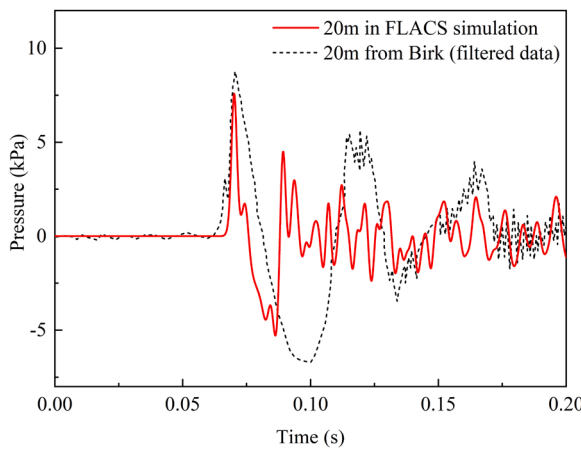


Fig. 3. Birk's test No. 02–01 pressure-time profile at 20 m (experiment & CFD simulation) (Li et al., 2021a).

BLEVE source. These include the tank failure pressure, temperature, tank size and structure dimension, etc. as listed in Table 2. An upper and a lower limit are set for each parameter and random values are sampled separately to form a BLEVE case. In total, 489 cases are generated, including 255 butane and 234 propane cases, respectively. The setting of used variables is described in detail as follows. For BLEVE source

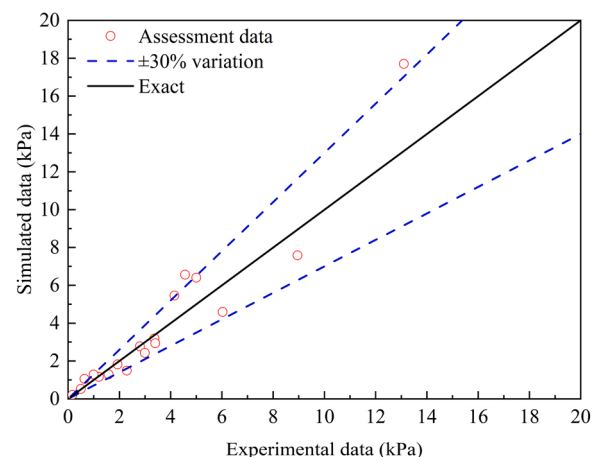


Fig. 4. The scatter plot of FLACS simulations and experimental data (Li et al., 2021a).

parameters, the same settings as those used in the open-space BLEVE study in Li et al. (2021a), are used. For example, tank failure pressure and temperature are essential parameters for determining the BLEVE energy. We set the failure pressure to be between the minimum experimental pressure (500 kPa) and the critical pressure of the internal pressurised liquid (i.e., 3700 kPa for butane and 4200 kPa for propane). The failure temperature is also increased up to the critical temperature of the liquid to fully consider BLEVE under both the non-superheated and superheated status. BLEVE tanks in simulations are simplified to cuboid shapes to minimise the mass residual problem, as the grid meshing in FLACS is the block control volume (Gexcon, 2017). The volume of BLEVE tanks is assumed to vary from 10 m³ to 90 m³ based on the European manufacturing standard of LPG tanks (Kadatec, 2017). Considering the ground effect, the BLEVE height is sampled between 0 and 2 m. A single rigid structure is modelled with varying dimensions to fully study its effect on blast wave propagation, i.e., reflection, diffraction, and pressure relief. The smallest structure is 3 m in width, 0.4 m in thickness and 3 m in height, while the largest one has the corresponding dimensions of 18 m, 3 m and 18 m, respectively. The distance between the BLEVE centre and the structure centre varies from 5 m to 20 m along the BLEVE wave propagation direction (i.e., x-direction). Fig. 6 shows a typical blast wave propagation of BLEVE with the presence of an obstacle, in which both the reflection and diffraction of the wave occurred. To thoroughly study the effect of the obstacle existence, 27 monitoring points (sensors) are placed on the three

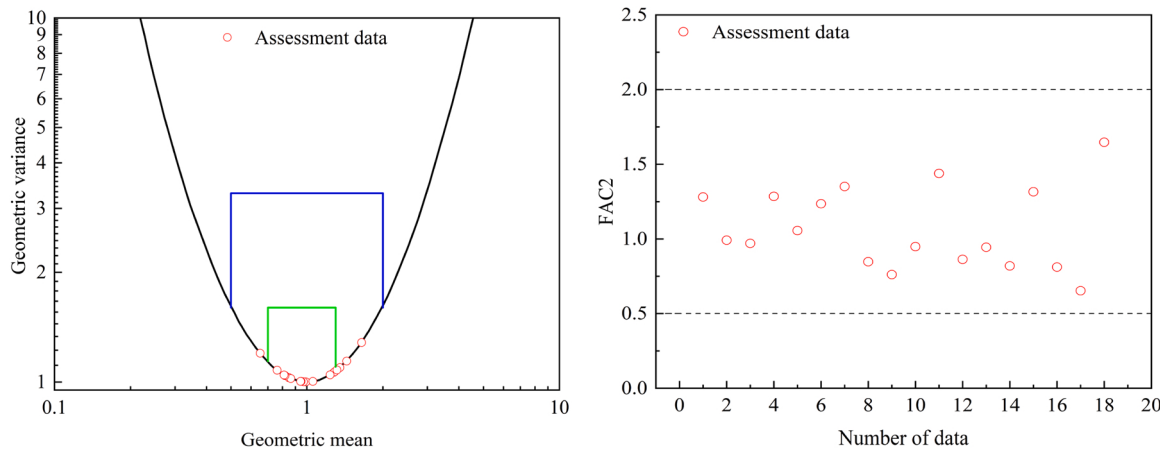


Fig. 5. The parabola plot (left) (Li et al., 2021a) and FAC2 plot (right) of FLACS simulations.

Table 2
A list of variables and their value ranges used to generate BLEVE simulations.

Variable	Value	
	Butane	Propane
Tank failure pressure (kPa)	500–3700	500–4200
Tank length (m)	0.2–10	
Tank width (m)	0.2–3	
Tank height (m)	0.2–3	
Liquid fill level (%)	10–90	
Liquid status	superheated or non-superheated	
Liquid temperature (°C)	1–152	1–96
Vapour temperature (°C)	1–304	1–192
Vapour height (m)	Calculated	
BLEVE height (m)	0–2	
Obstacle distance (m)	5–20	
Obstacle angle (°)	0–45	
Obstacle width (m)	3–18	
Obstacle height (m)	3–18	
Obstacle thickness (m)	0.4–3	
Obstacle wall of sensor	front, back, or side	
Sensor location x-axis	Manually chosen	
Sensor location y-axis	Manually chosen	
Sensor location z-axis	Manually chosen	
Output pressure (kPa)	0–600	
Output impulse (Pa·s)	0–1400	

obstacle surfaces, i.e., front, rear, and side surfaces, resulting in 9 sensors on each surface as shown in Fig. 7. Note that the training and testing of machine learning models will be based on the reflected BLEVE loadings (pressure or impulse) extracted from these sensors, that is, each BLEVE

case gives 27 outputs corresponding to 27 sensors. The 489 BLEVE cases result in a total of 13203 data instances for the training and evaluation of machine learning models, which are discussed in the next section.

3. Methodology and implementation of Transformer

3.1. The methodology of the Transformer model

Transformer networks are the state-of-the-art models for complex artificial intelligence tasks including natural language processing (Vaswani et al., 2017) and computer vision (Dosovitskiy et al., 2020). Transformers are designed to process sequential data, such as sentences consisting of a sequence of words. Based on the self-attention mechanism (Vaswani et al., 2017), Transformers learn global representations by differentially weighting each part of data, e.g., encoding sentences by weighting each of the words embedding (token). Transformers can also be applied to data that is not naturally sequential, e.g., Vision Transformer (Dosovitskiy et al., 2020) converts an image to a sequence of patches and achieves better results than convolutional networks in vision tasks.

In this study, the simulated BLEVE data are presented in tabular format, where a row represents a data instance, and a column represents a variable (feature). Transformers are not directly applicable to tabular data due to the lack of sequential order and multi-dimensional embedding of features. The Feature-Tokenizer Transformer (FT-Transformer) (Gorishniy et al., 2021) is a simple variant of the original Transformer (Vaswani et al., 2017) for tabular data and will be adapted for BLEVE loading prediction in this study.

The FT-Transformer consists of three components, namely feature

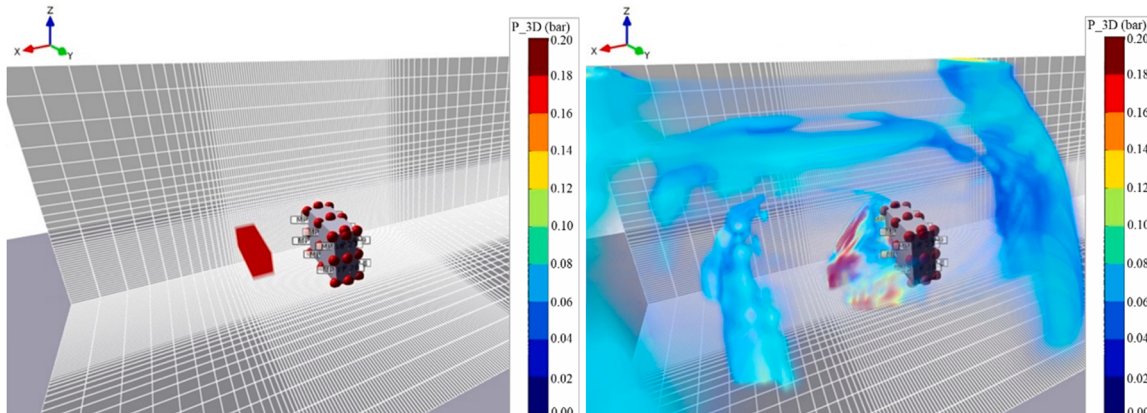


Fig. 6. An example of BLEVE blast wave propagation with a rigid obstacle.

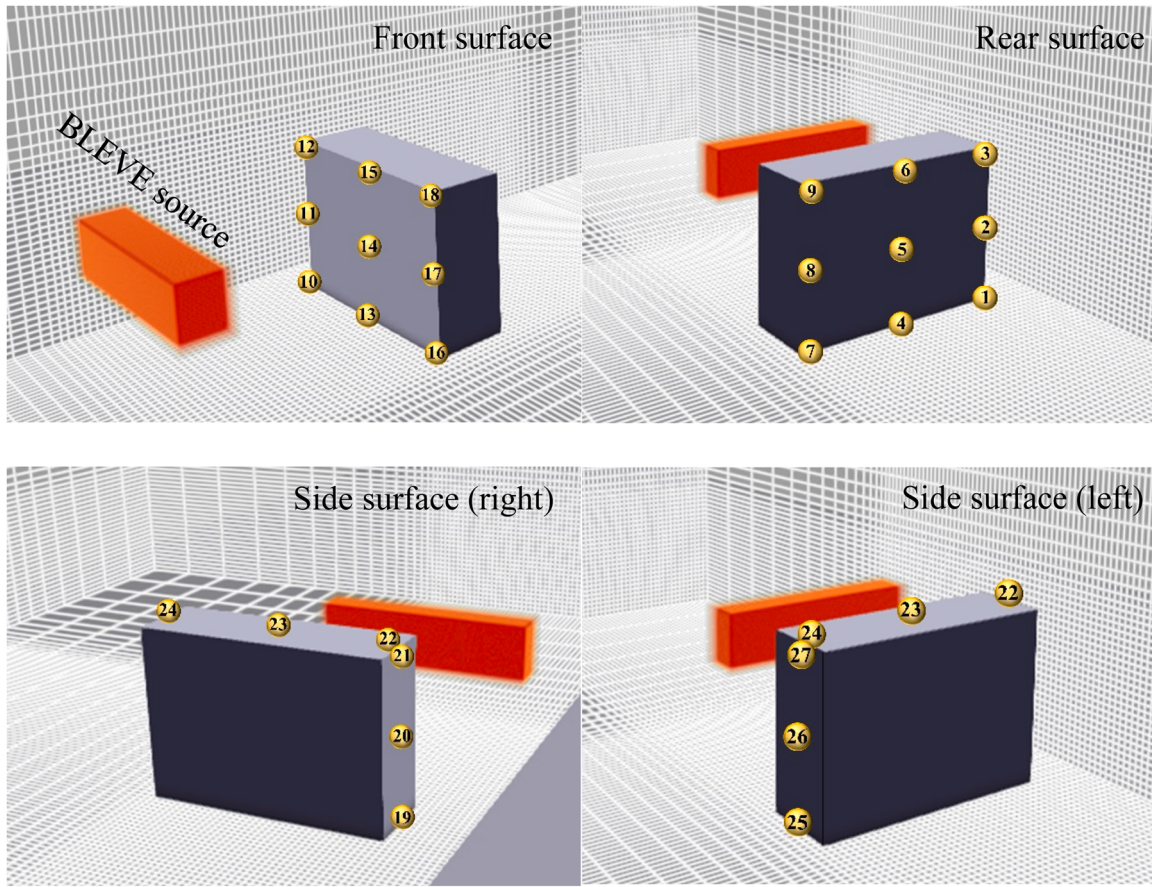


Fig. 7. The illustration of 27 sensors on the obstacle, where 9 sensors are evenly distributed on each of the front, rear, and side surfaces.

tokenizer, Transformer layers, and prediction head, as shown in Fig. 8. Simply speaking, the FT-Transformer converts all features to embeddings, updates embeddings with a stack of Transformer layers, and makes predictions based on the embedding of the last layer. Next, we introduce each component in detail.

3.1.1. Feature tokenizers

The feature tokenizer converts a 1-dimensional feature x_i to a

d -dimensional feature embedding T_i (vector) via a linear projection as follows:

$$T_i = x_i \bullet W_i + b_i \quad (4)$$

where $W_i \in R^d$ and b_i are learnable weights and bias for the i -th feature. Categorical features follow the same process by first converting to numerical features using integer encoding.

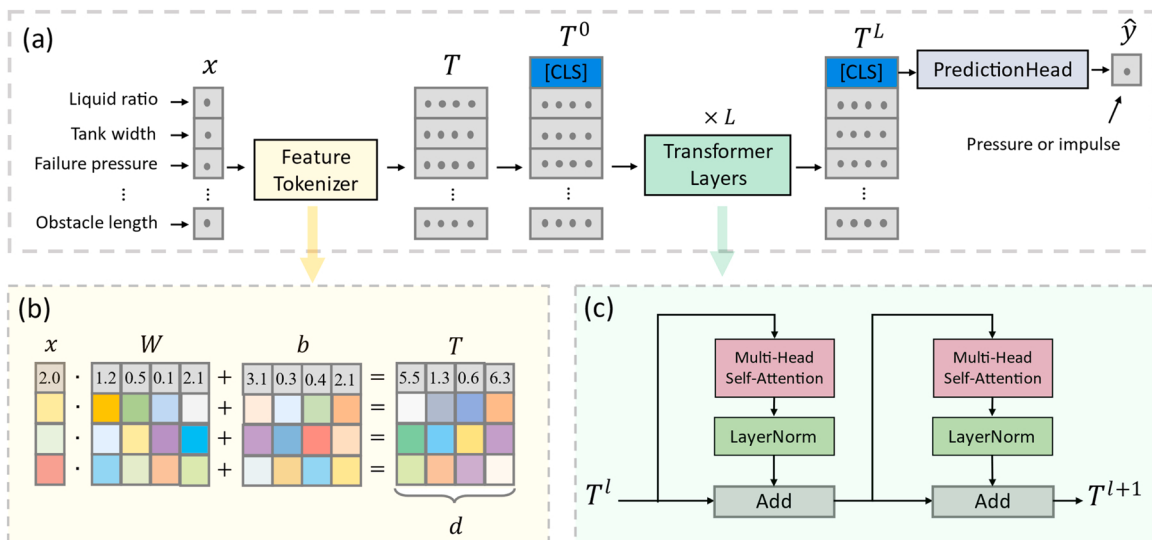


Fig. 8. The flowchart of the FT-Transformer model. (a) The overall architecture; (b) The feature tokenizer module; (c) The Transformer module.

3.1.2. Transformer layers

The Transformer layers are the core building blocks of Transformer networks. Each Transformer layer is made of a multi-head self-attention (MHSA) (Vaswani et al., 2017) module that transforms feature embeddings T (tokens) by aggregating tokens from the previous layer and a feed-forward neural network module that transforms each embedding individually. By stacking L Transformer layers, the network learns, for each feature, a latent embedding that captures long-range dependencies among tokens. Note that a special learnable [CLS] token (Devlin et al., 2018) is appended to T , as shown in Fig. 8 and this [CLS] token will aggregate relevant information from all feature tokens and represent the data instance as a whole. Prediction based on [CLS] token will therefore not bias to any particular feature. Assuming the l -th Transformer layer is a function f^l , the sequence of Transformer layers can be formulated as:

$$T^l = f^l(T^{l-1}) \text{ where } T^0 = \text{concatenate}[[\text{CLS}], T]. \quad (5)$$

3.1.3. Prediction head

The prediction head applies a simple transformation on the final representation of the [CLS] token:

$$\hat{y} = \text{Linear}\left(\text{ReLU}\left(\text{LayerNorm}\left(T_{[\text{CLS}]}^L\right)\right)\right). \quad (6)$$

The Transformer model is trained using supervised learning, that is, the model is iteratively updated to minimise an objective loss function. The Mean Squared Error (MSE) is used in this study, and it is defined as:

$$MSE = \frac{1}{N} \sum_{i=1}^N (y_i - \hat{y}_i)^2, \quad (7)$$

where y_i is the ground truth of the i -th data instance and N is the total number of data instances.

3.2. Implementation details and evaluation metrics

3.2.1. Data preparation

The BLEVE dataset consists of 489 simulated BLEVE cases, and it is randomly split into the training set and testing set with a ratio of 8:2. Note that each case consists of 27 monitoring points, and thus there are 10557 and 2646 data points in the training and testing sets, respectively. The variable ranges for the training and testing data are statistically equal to the ranges of the whole dataset (shown in Table 2) from which they are stochastically drawn. 20 % of the training set is further split out as the validation set for tuning hyperparameter. The quantile transformation with normal distribution is applied to both input x and target y . While the normalisation of x benefits the training stability, the target normalisation improves the prediction accuracy.

3.2.2. Training and hyperparameter tuning

The Transformer network is trained with the AdamW (Loshchilov and Hutter, 2018) optimiser with a batch size of 256. The performance on the validation set is monitored during the training and used for early stopping, that is, the model is trained until the validation performance does not improve for 16 epochs consecutively. The Transformer architecture-related hyperparameters, such as the number of layers L and the token dimensions d , as well as model training-related hyperparameters, such as learning rate and weight decay, are carefully tuned to obtain the best prediction performance. Bayesian optimisation-based hyperparameter search (Akiba et al., 2019) is performed to find optimal hyperparameters, which is reported to be better than grid search and random search (Turner et al., 2021; Bergstra and Bengio, 2012). The search budget is limited to 100 trials, i.e., 100 combinations of hyperparameters will be evaluated and the best performing set of values will be used. Two sets of hyperparameters will be tuned separately for pressure and impulse prediction.

3.2.3. Evaluation metric

Predicting continuous quantities, such as pressure and impulse, is a regression problem for which there is no precise definition of correct or incorrect predictions. The error, or deviation of prediction from ground truth, can be quantified to measure the correctness. Different evaluation metrics that quantify the error from various perspectives may not agree with each other in certain cases (shown in Figs. 8&9). For a thorough evaluation, three error metrics are utilised, including Root Mean Square Error (RMSE), Mean Absolute Percentage Error (MAPE), and Coefficient of Determination (R^2 -squared, R^2).

Given ground truth y and prediction \hat{y} , RMSE quantifies the standard deviation of the prediction error as follows:

$$RMSE = \sqrt{\frac{1}{N} \sum_{i=1}^N (y_i - \hat{y}_i)^2}, \quad (8)$$

where N is the number of data points. RMSE is lower bounded by zero and the smaller the better. MAPE quantifies a relative percentage error of prediction to the ground truth and can be written as:

$$MAPE = \frac{1}{N} \sum_{i=1}^N \left| \frac{y_i - \hat{y}_i}{y_i} \right|. \quad (9)$$

MAPE is also bounded by zero and the smaller the better. R^2 quantifies the degree of linear correlation between prediction and ground truth, and it is defined as:

$$R^2 = 1 - \frac{\sum_{i=1}^N (y_i - \hat{y}_i)^2}{\sum_{i=1}^N (y_i - \bar{y})^2}, \quad (10)$$

where $\bar{y} = \sum_{i=1}^N y_i / N$ is the mean of ground truth, e.g., the mean pressure of all data instances. R^2 measures the deviation from a global distribution point of view and typically ranges from 0 to 1 (R^2 becomes negative if the prediction is even worse than a constant \bar{y}). R^2 is the larger the better.

4. Experimental results

The experimental results are split into three subsections: (1) a comparative study is first conducted to show that the developed Transformer network outperforms the widely used MLP for BLEVE loading prediction, (2) an in-depth error analysis of the Transformer model is then performed to evaluate its behaviour in terms of parameters of interest, including the scale of blast loading and the location of monitor point on the structure, and (3) a prediction of pressure-time profile is eventually generated for a detailed characterisation of BLEVE loads.

4.1. Comparison between Transformer and MLP

The Multi-Layer Perceptron (MLP) is the most widely used machine learning model for blast loading prediction. As a baseline, an MLP model is also developed, following the same training and tuning protocol as of Transformer for a fair comparison. The experiment is repeated 10 times to remove the random effect and the mean performance with the standard deviation is reported on the test set.

Table 3 presents the prediction performance for both pressure and impulse. The Transformer model consistently outperforms MLP with a clear margin for all three evaluation metrics including RMSE, MAPE and R^2 . For example, in terms of MAPE, Transformer reduces the prediction error of MLP by 25.6 % and 30.6 % for peak pressure and impulse, respectively. This result suggests that Transformer is more suitable than the commonly used MLP for BLEVE load prediction. Furthermore, the used Transformer hyperparameters for pressure prediction and impulse prediction are summarised in Table 4. These hyperparameters are

Table 3

Prediction performance of MLP and Transformer for BLEVE pressure and impulse.

Target	Model	Metric		
		RMSE	MAPE	R ²
Pressure	MLP	16.82 ± 0.016	0.180 ± 0.008	0.858 ± 0.027
	Transformer	11.64 ± 0.006	0.134 ± 0.007	0.933 ± 0.007
Impulse	MLP	36.92 ± 2.622	0.196 ± 0.014	0.920 ± 0.012
	Transformer	30.30 ± 0.960	0.136 ± 0.006	0.947 ± 0.003/td>

Note: in terms of RMSE, the unit of pressure is kPa and impulse is Pa·s.

automatically tuned with the Bayesian optimisation-based search method, and the small difference between the two sets of hyperparameters shows a certain degree of robustness of the Transformer model. As a reference, the tuned MLP model specifications are also presented in Table 5. As shown, the tuned MLP architecture is comparable to that of Transformer in terms of the depth and width, and the advantage of Transformer comes from primarily the computation mechanism in each layer, i.e., the self-attention module.

4.2. Analysis of the Transformer model prediction

With the configuration presented in Table 4, two Transformer models are trained for peak pressure and impulse prediction, respectively. The training strategy follows the same one used for hyperparameter tuning. That is, the model is trained on the training set and its performance on the validation set is monitored for early stopping with the patience of 16 epochs. The trained model is then applied to the testing set to make the final prediction. Next, we conduct a rigorous performance analysis of Transformer prediction for a better understanding of the model behaviour.

4.2.1. Overview with scatter plots

The scatter plot between the ground truth (produced by FLACS simulation) and Transformer prediction is presented in Fig. 9 and Fig. 10, where x-axis and y-axis represent target and prediction, respectively. The red dashed line represents a perfect model, i.e., the prediction is the same as the target. Each blue point denotes test data and a linear regression line (blue) that best fits these points (95% confidence interval) is also shown. In each plot, quantitative performance evaluations (MAPE and R²) of corresponding subsets are also given.

Fig. 9 shows the scatter plots for BLEVE pressure prediction over three ranges: (a) 0–600 kPa, (b) 0–30 kPa, and (c) 50–150 kPa. Fig. 9(a) covers the entire range of peak pressure presented in the test data. It is observed that points are centred around the perfect red line and the regression blue line is almost identical to the red one, which indicates that the Transformer predictions are fairly accurate. Fig. 9(b) presents the zoom-in scatter plot for pressures from 0–30 kPa. The points are visually more spread out, which is demonstrated by the decrease of the R² value from 0.936 to 0.872. The relative error MAPE, on the other

hand, shows that the model has similar performance in (a) and (b). Fig. 9(c) presents the zoom-in scatter plot for pressure from 50–150 kPa, and similar behaviour is observed that the absolute error R² is larger while the relative error is close. The inconsistency is due to the inherent difference between the two metrics, i.e., they behave differently when the scale of the actual target changes. In practice, it is suggested that R² should be used for the comparison of models and MAPE should be used for the quantification of errors, as the former provides a robust statistical measurement of accuracy while the latter contains richer physical meanings.

Fig. 10 shows the scatter plots for BLEVE impulse prediction over three ranges: (a) covers the whole impulse range from 0 to 1400 Pa·s, (b) 0–100 Pa·s, and (c) 200–600 Pa·s. Like the pressure prediction, the Transformer prediction is overall qualitatively and quantitatively accurate, as shown by the scatter plots and evaluation metrics. It is observed, however, that the model tends to underestimate the peak impulse, especially when the impulse is larger than 800 Pa·s. The reason could be that there is very limited data with large impulse and the model is trained to bias towards low impulse. Such a problem can be addressed by adding more training data of large impulse.

4.2.2. Error breakdown based on target range

To thoroughly investigate the predictive behaviour of the Transformer model, we break down the prediction error with respect to the target output value and study if the model is biased to certain scales of the BLEVE explosion. Specifically, test data is split into several groups based on the target output and the error distribution is investigated for each group. To be concise, only the relative error MAPE is used for this analysis.

Table 6 shows the error breakdown for pressure prediction. As indicated by the mean relative error of each group, the Transformer model produces relatively higher error rates for the group of small pressures ($P \leq 10$ kPa) and the group of large pressures ($P > 100$ kPa). For small pressures (≤ 10 kPa), the reason should be that the absolute square error MSE is biased to large values. For large pressures, reasons are two-fold: from machine learning point of view, data with large pressures are limited, and from blast engineering point of view, large pressures generally appear in the near-field of the blast source, which is known to be difficult to predict. Overall, the Transformer model achieves 13.4 % relative error for peak pressure prediction, in which more than 50 % of test data are predicted with less than 10% error and more than 90 % of data have less than 30 % error, for all target pressure

Table 4

The tuned Transformer model specification for pressure and impulse prediction.

Hyperparameter	Pressure	Impulse
Number of layers	4	4
Token dimensions	344	432
Attention heads	8	8
Attention scaling factor	2.37	3.93
Activation function	ReLU	ReLU
Dropout probability	0.09	0.08
Learning rate	9.49e-5	7.09e-5
Weight decay	1.05e-5	2.72e-5
Optimiser	AdamW	AdamW
Batch size	256	256

Table 5

The tuned MLP model specification for pressure and impulse prediction.

Hyperparameter	Pressure	Impulse
Number of layers	4	5
Number of neurons	[312, 304, 304, 252]	[495, 416, 416, 416, 349]
Activation function	ReLU	ReLU
Dropout probability	0.06	0.00
Learning rate	3.71e-3	5.26e-3
Weight decay	0.00	6.83e-4
Optimiser	AdamW	AdamW
Batch size	256	256

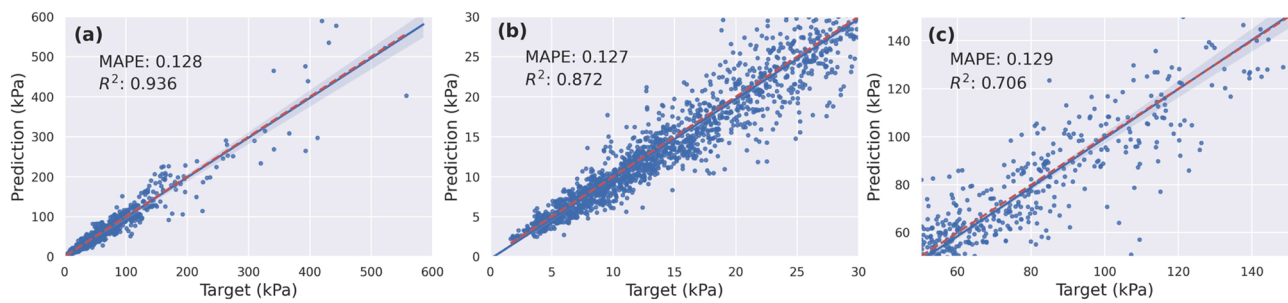


Fig. 9. Pressure prediction scatter plots of actual target and prediction, ranging from (a) 0–600 kPa; (b) 0–30 kPa; (c) 50–150 kPa.

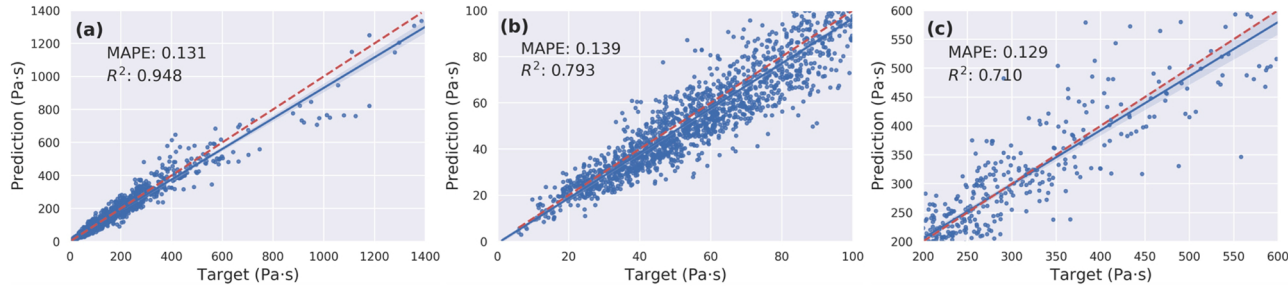


Fig. 10. Impulse prediction scatter plots of actual target and prediction, ranging from (a) 0 – 1400 Pa·s; (b) 0 – 100 Pa·s; (c) 200 – 600 Pa·s.

Table 6
Pressure prediction error breakdown with respect to the target range.

Target pressure range (kPa)	Number of data	Mean error (%)	Data ratio within relative error (%)			
			E ≤ 10	E ≤ 20	E ≤ 30	E ≤ 50
			10	20	30	50
P ≤ 10	634	13.5	50.5	74.2	90.9	98.6
10 < P ≤ 30	1056	12.1	52.4	83.6	93.4	98.4
30 < P ≤ 50	444	12.4	52.3	82.0	93.7	98.9
50 < P ≤ 100	346	11.8	55.5	84.4	93.9	99.1
P > 100	162	13.6	51.9	71.0	90.8	99.4

Table 7
Impulse prediction error breakdown with respect to the target range.

Target impulse range (Pa·s)	Number of data	Mean error (%)	Data ratio within relative error (%)			
			E ≤ 10	E ≤ 20	E ≤ 30	E ≤ 50
			10	20	30	50
I ≤ 50	692	16.2	40.2	72.1	87.7	96.5
50 < I ≤ 100	886	12.8	49.0	79.5	93.7	98.7
100 < I ≤ 200	684	12.0	47.8	83.2	96.4	99.6
200 < I ≤ 300	206	11.0	49.5	81.5	95.6	100
I > 300	168	14.6	33.3	73.2	94.6	100

ranges.

Table 7 presents the error breakdown for impulse prediction. Similar patterns are observed compared to pressure prediction in Table 6. That is, the prediction is less accurate when the target impulse is either very small ($I \leq 50$ Pa·s) or very large ($I > 300$ Pa·s). Compared to pressure prediction, the model produces less highly accurate predictions ($E \leq 10$) but more "reasonable" predictions ($E \leq 50$). In particular, the prediction errors are capped at 50 % for all test data of impulse larger than 300 Pa·s.

4.2.3. Error breakdown based on sensor location on the obstacle

Next, the prediction performance of the Transformer model in terms of the sensor location on the obstacle is studied. Three parts of the

Table 8
Prediction error of pressure on different wall faces.

MAPE	Back wall	Front Wall	Side wall
	Pressure	0.114	0.127
Impulse	0.123	0.128	
	0.155		

obstacle are considered: the back wall, front wall, and side wall, where 9 sensors at different locations on the wall (monitoring points in FLACS simulation) are evenly distributed on each side of the wall. We first study the model behaviour with respect to each wall and then analyse the prediction for individual sensors.

Table 8 shows the model performance in terms of MAPE based on each side of the obstacle wall, in which the result is the average of all sensors on that side of the obstacle. The model is slightly better in predicting pressure on the front wall and less accurate for the back wall, and this is likely due to the difficulty of modelling the diffraction of the blast wave, for both CFD and machine learning models.

Fig. 11 presents the pressure prediction at typical sensor locations on each face of the obstacle (refer to Fig. 6 for sensor locations). The plots are obtained by separating test data into groups, where each group contains data points from one sensor only. Data in each group are then sorted based on the target value and plotted with the corresponding prediction. Note that the horizontal axis in Fig. 11 represents the index of sorted test data, and therefore there is no temporal relationship. The vertical axis indicates the range of pressure at each sensor location considered in this study, and as expected, the front wall bears a much larger peak pressure than the back wall, e.g., the peak pressure of sensor 5 at the centre of the back wall is up to 30 kPa, while that of sensor 14 at the centre of front wall is up to 400 kPa for the BLEVE scenarios considered in the study. The model makes relatively better predictions on the front face of the obstacle (Fig. 11(b)). In particular, using the centre point of each wall as an example (the middle row of Fig. 11), it shows that the predictions (red line) start "vibrating" around the target (blue line) even when the target is small for the back wall. In contrast, the prediction on the front wall is better aligned with the target, especially in the lower end of the target.

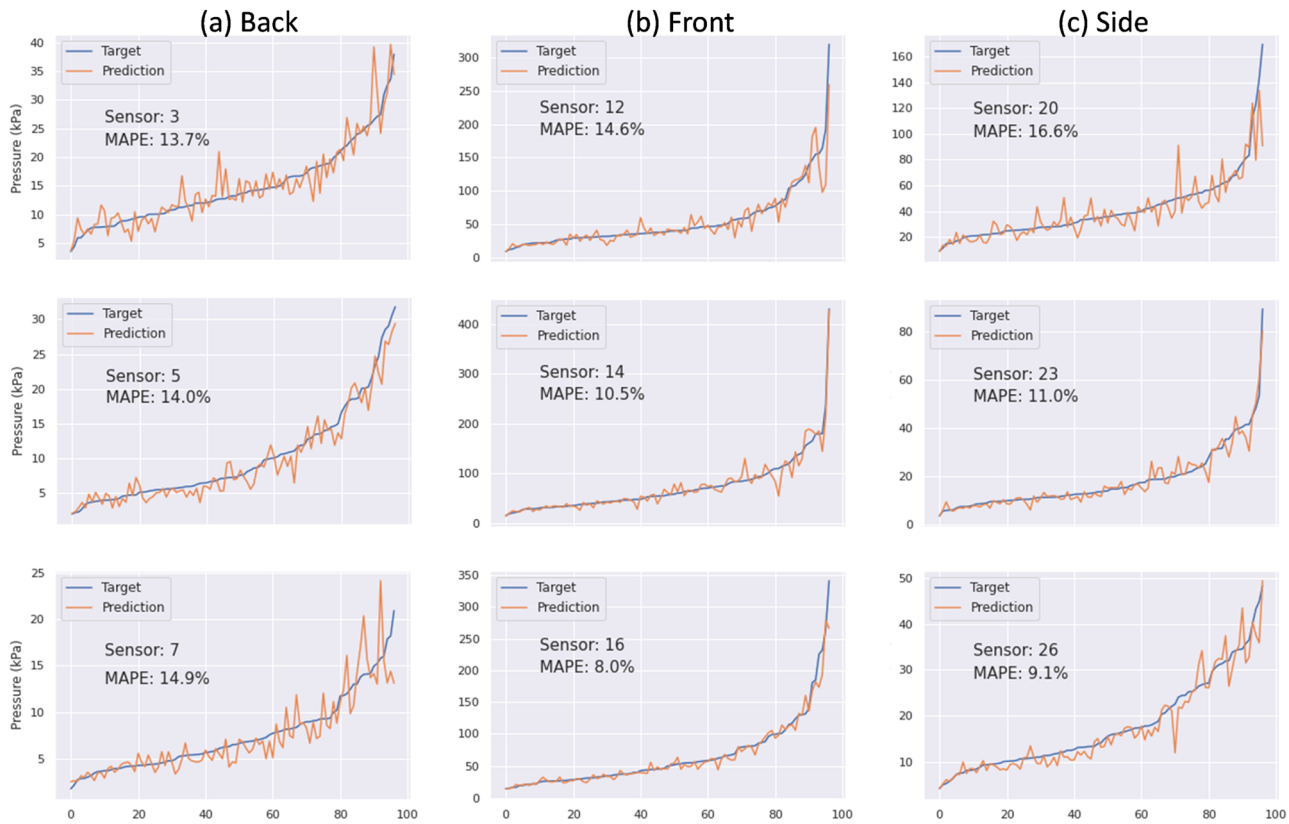


Fig. 11. Pressure prediction plots based on typical sensors on each side of the obstacle: (a) back; (b) front; (c) side faces. Note that the horizontal axis is the index of sorted test data and hence no temporal relationship presents.

4.3. Prediction of pressure-time history

The developed Transformer model is demonstrated to be capable of predicting peak pressure and impulse accurately at different locations on different faces of wall. However, they are not enough to fully characterise the blast load. A complete BLEVE pressure-time profile is known to contain several peaks (shown in Fig. 2). The first peak is generated by the leading shock wave from exploding vapour, and it is followed by a negative phase and a second shock produced by an overexpansion followed by a recompression of the released vapour (Baker et al., 2012). There is often a third peak for BLEVE which is explained by some researchers being due to the extra energy from liquid flashing (Li and Hao, 2020; Birk et al., 2007). Despite these many peaks, the leading peak is the largest and it is also reported in (Li and Hao, 2020) that the existing CFD approaches, including FLACS used in this study, cannot model the second and the third peaks very well. We therefore focus on the prediction of the first peak and the associated negative phase, which are

larger than the second and third peaks and have the most detrimental effects on structures. To fully characterise the pressure-time history for this period, seven critical parameters are needed, namely positive peak pressure (P_p^+), negative peak pressure (P_p^-), arrive time (t_a), positive peak time (t_p^+), negative peak time (t_p^-), positive duration (t_d^+), and negative duration (t_d^-). These parameters and their relationship are illustrated in Fig. 12.

Seven Transformer models are trained and tuned for these parameters respectively, using the same training and hyperparameter tuning protocols described in Section 3.2. The trained models are applied to the testing dataset and the performance in terms of relative error MAPE is presented in Fig. 13. The widely used MLP model is also added for a complete comparison. It shows that Transformer outperforms MLP, achieving relative errors less than 20 %, on all seven outputs. The predicted arrival time t_a has the lowest error of less than 5 %. The predicted negative pressure duration t_d^- shows a significantly larger error than that of the positive pressure duration t_d^+ , demonstrating the difficulty of accurately modelling the complex interaction between the structure and blast wave. Overall, the Transformer model shows its superior capability in predicting these critical blast wave parameters.

Next, the predictions for seven critical parameters are combined to form the pressure-time history of BLEVE. Specifically, given the input variables of a BLEVE case (shown in Table 2), the Transformer models are used to predict critical parameters separately and straight lines are used to approximate the underlying pressure curve. Fig. 14 presents the pressure-time history for three BLEVE cases with data from FLACS simulation, MLP prediction, and Transformer prediction. The three cases are selected so that the obtained pressures are small, medium, and large. For each BLEVE case, the pressure-time profiles at the centre of front face, back face, and right-side of the wall (correspond to sensors 14, 5 and 20 in Fig. 7) are presented.

There are several notable observations in Fig. 14. (1) Compared to

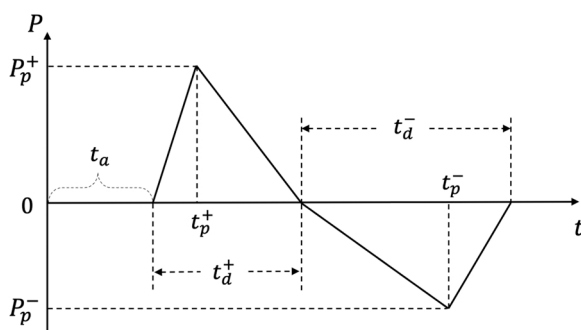


Fig. 12. The characterisation of BLEVE blast loads with seven critical parameters.

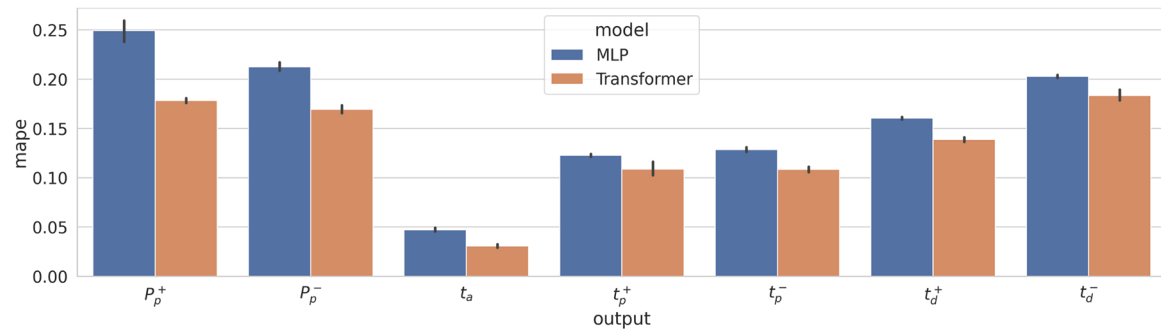


Fig. 13. Testing performance on seven critical blast load parameters.

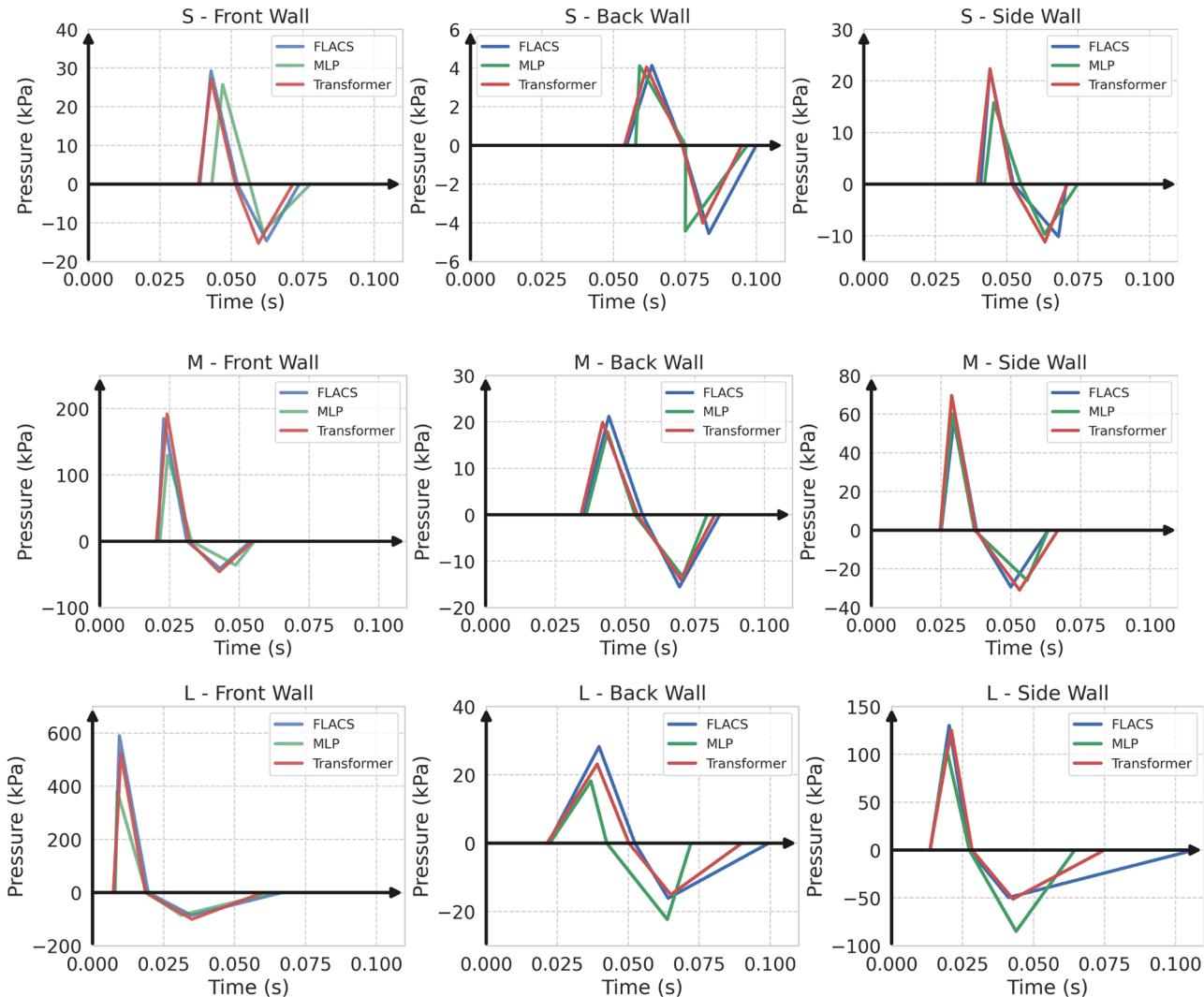


Fig. 14. Comparison of predicted reflected Pressure - Time histories with different methods from small (S), medium (M), and large (L) BLEVEs.

MLP, Transformer aligns better with FLACs in terms of pressure peaks and peak times, which is well expected. (2) Compared to the positive pressure phase, it is more challenging to predict BLEVE loads in the negative phase, especially the duration of negative pressure. (3) Pressure peaks are well captured by Transformer, especially for those on the front face and side face of the wall due to relatively simple physical phenomena (i.e., incidence & reflection), while there is a slight mismatch in the predicted pressure time history on the back wall. Note that this observation is aligned with the results in Table 8 that the

prediction error on the back face is slightly larger than the other faces, which makes sense due to the complex diffraction waves on the rear side of the wall. (4) The front wall peak pressure is the largest since the blast wave is intensified by superposition of reflected blast wave, and it is around $10\times$ to $20\times$ of the pressure on the back face due to the shadowing effect of the wall and energy loss in the diffraction process (note that the thickness of the structure is up to 3 m). (5) The positive peak pressure is significantly larger than the negative peak on the front wall, while the difference of these two peaks is marginal on the back side of

the wall. (6) When the pressure is large, the negative phase is evidently longer than the positive phase, as observed in the large-scale case (bottom row of Fig. 14). Note that these findings are based on the data from the centres of front, back, and right-side faces of the obstacle, and may not apply to some other monitoring points, such as those on the boundary of the wall. Overall, it is demonstrated that Transformer can well predict the loading-time history on the structure. It is therefore believed that Transformer can be used as an effective tool for BLEVE blast load prediction.

5. Conclusion

In this study, BLEVE loading prediction with the presence of a rigid obstacle is investigated using CFD and machine learning. The validated CFD model based on FLACS is utilised to generate 489 BLEVE cases, including butane and propane, for the training and evaluation of machine learning models. Instead of using commonly adopted multi-layer perceptron (MLP) models, state-of-the-art Transformer networks are studied for the prediction of a complete set of critical parameters related to BLEVE loads. It is demonstrated with a substantial amount of simulation data that Transformers lead to more accurate predictions of BLEVE loads on structures than MLP models.

An in-depth analysis of Transformer model, using pressure and impulse predictions, shows that the model performs equally well for different scales of BLEVEs, with a slightly worse performance for extreme cases. It also shows that it is more difficult for Transformers to accurately predict BLEVE loading on the back wall of structures, possibly due to more complex wave diffractions and much smaller scale of loads.

Despite it has been commonly used in many blast engineering applications, this study shows that MLP gives less accurate predictions of BLEVE loads on structures as compared to Transformers, indicating more attentions should be paid to advanced machine learning models, which are likely to generate more accurate predictions. The developed Transformer in this study can be used as a surrogate model of the computationally expensive CFD to generate abundant data for the analysis of BLEVE loads on structures for structural response predictions.

Declaration of Competing Interest

The authors declare that they have no known competing financial interests or personal relationships that could have appeared to influence the work reported in this paper.

References

- Abbasi, T., Abbasi, S., 2007. The boiling liquid expanding vapour explosion (BLEVE): Mechanism, consequence assessment, management. *J. Hazard. Mater.* 141 (3), 489–519.
- T. Akiba, S. Sano, T. Yanase, T. Ohta, and M. Koyama, 2019. Optuna: A next-generation hyperparameter optimization framework, In: Proceedings of the 25th ACM SIGKDD International Conference on Knowledge Discovery & Data Mining, pp. 2623–2631.
- W.E. Baker, P. Cox, J. Kulesz, R. Strehlow, and P. Westine, *Explosion hazards and evaluation*. Elsevier, 2012.
- Bergstra, J., Bengio, Y., 2012. Random search for hyper-parameter optimization. *J. Mach. Learn. Res.* 13 (2).
- Birk, A., Cunningham, M., 1994. The boiling liquid expanding vapour explosion. *J. Loss Prev. Process Ind.* 7 (6), 474–480.
- Birk, A., VanderSteen, J., 2006. On the transition from non-BLEVE to BLEVE failure for a 1.8 m³ propane tank.
- Birk, A., Davison, C., Cunningham, M., 2007. Blast overpressures from medium scale BLEVE tests. *J. Loss Prev. Process Ind.* 20 (3), 194–206.
- CCPS , 2011. Guidelines for Vapor Cloud Explosion, Pressure Vessel Burst, BLEVE, and Flash Fire Hazards, (August 2010)," *Process Safety Progress*, vol. 30, no. 2, p. 187.
- Devlin, J., Chang, M.-W., Lee, K., Toutanova, K., 2018. Bert: Pre-training of deep bidirectional transformers for language understanding, arXiv preprint arXiv: 1810.04805, 2018.
- Dosovitskiy, A., et al., 2020. An image is worth 16×16 words: Transformers for image recognition at scale, arXiv preprint arXiv:2010.11929.
- Gebreslassie, M.G., Tabor, G., Belmont, M.R., 2012. CFD simulations for sensitivity analysis of different parameters to the wake characteristics of tidal turbine. 2017 Gexcon, 2017. "FLACS v10.7 User's Manual, Norway.
- Gorishniy, Y., Rubachev, I., Khruklov, V., Babenko, A., 2021. Revisiting deep learning models for tabular data. *Adv. Neural Inf. Process. Syst.* 34, 18932–18943.
- Hansen, O.R., Kjellander, M., 2016. CFD modelling of blast waves from BLEVEs, (in English). *Chem. Eng. Trans.* 48, 199–204. <https://doi.org/10.3303/CET1648034>.
- Hao, H., Hao, Y., Li, J., Chen, W., 2016. Review of the current practices in blast-resistant analysis and design of concrete structures. *Adv. Struct. Eng.* 19 (8), 1193–1223.
- Hemmatian, B., Planas, E., Casal, J., 2015. Fire as a primary event of accident domino sequences: the case of BLEVE. *Reliab. Eng. Syst. Saf.* 139, 141–148. <https://doi.org/10.1016/j.ress.2015.03.021>.
- Hemmatian, B., Planas, E., Casal, J., 2017. Comparative analysis of BLEVE mechanical energy and overpressure modelling. *Process Saf. Environ. Prot.* 106, 138–149. <https://doi.org/10.1016/j.psep.2017.01.007>.
- Hemmatian, B., Casal, J., Planas, E., Hemmatian, B., Rashtchian, D., 2020. Prediction of BLEVE mechanical energy by implementation of artificial neural network. *J. Loss Prev. Process Ind.* 63, 104021.
- A. Hutama, Simulation of BLEVEs in Unconfined and Confined Areas Using FLACS, University of Stavanger, Norway, 2017.
- D. Johnson and M. Pritchard, "Large scale experimental study of boiling liquid expanding vapour explosions (BLEVEs)," in Gastech 90, International LNG/LPG Conference & Exhibition, 1990.
- Kadatec, 2017. LPG Road Tankers & ISO Tank Containers, V9 09. (accessed).
- Launder, B.E., Spalding, D.B., 1983. The numerical computation of turbulent flows. *Numerical Prediction of Flow, Heat Transfer, Turbulence and Combustion*. Elsevier, pp. 96–116.
- Li, J., Hao, H., 2019. Numerical and analytical prediction of pressure and impulse from vented gas explosion in large cylindrical tanks. *Process Saf. Environ. Prot.* 127, 226–244.
- Li, J., Hao, H., 2020. Numerical study of medium to large scale BLEVE for blast wave prediction. *J. Loss Prev. Process Ind.* 104–107.
- Li, J., Hao, H., 2021. Numerical simulation of medium to large scale BLEVE and the prediction of BLEVE's blast wave in obstructed environment. *Process Saf. Environ. Prot.* 145, 94–109. <https://doi.org/10.1016/j.psep.2020.07.038>.
- Li, J., Hao, H., Shi, Y., Fang, Q., Li, Z., Chen, L., 2018. Experimental and computational fluid dynamics study of separation gap effect on gas explosion mitigation for methane storage tanks. *J. Loss Prev. Process Ind.* 55, 359–380.
- Li, J., Li, Q., Hao, H., Li, L., 2021a. Prediction of BLEVE blast loading using CFD and artificial neural network. *Process Saf. Environ. Prot.* 149, 711–723.
- Li, J., Hao, H., Chen, W., Cheng, R., 2021b. Calculation of BLEVE energy and overpressures inside a tunnel using analytical and CFD methods. *Tunn. Undergr. Space Technol.*, 104263 <https://doi.org/10.1016/j.tust.2021.104263>.
- Li, Q., Wang, Y., Shao, Y., Li, L., Hao, H., 2023. A comparative study on the most effective machine learning model for blast loading prediction: from GBDT to transformer. *Eng. Struct.* 276, 115310.
- Loshchilov, I., Hutter, F., 2018. Decoupled weight decay regularization. In: *Proceedings of the International Conference on Learning Representations*.
- P. Middha, O.R. Hansen, M. Groethe, and B.J. Arntzen, 2007. Hydrogen explosion study in a confined tube: FLACS CFD simulations and experiments, In: *Proceedings of 21st International Colloquium of Dynamics of Explosions and Reactive Systems*, Poitiers, France, 2007.
- Mitu, M., Prodan, M., Giurcan, V., Razus, D., Oancea, D., 2016. Influence of inert gas addition on propagation indices of methane-air deflagrations. *Process Saf. Environ. Prot.* 102, 513–522.
- Paltrinieri, N., Landucci, G., Molag, M., Bonvicini, S., Spadoni, G., Cozzani, V., 2009. Risk reduction in road and rail LPG transportation by passive fire protection. *J. Hazard. Mater.* 167 (1), 332–344. <https://doi.org/10.1016/j.jhazmat.2008.12.122>.
- Shi, Y., Hao, H., Li, Z.-X., 2007. Numerical simulation of blast wave interaction with structure columns. *Shock Waves* 17 (1), 113–133.
- Spoelstra, M., Mahesh, S., Kooi, E., Heezen, P., 2015. Domino effects at LPG and propane storage sites in the Netherlands. *Reliab. Eng. Syst. Saf.* 143, 85–90. <https://doi.org/10.1016/j.ress.2015.06.018>.
- Török, Z., Ajtai, N., Turcu, A.-T., Ozunu, A., 2011. Comparative consequence analysis of the BLEVE phenomena in the context on land use planning: case study: the Feyzin accident. *Process Saf. Environ. Prot.* 89 (1), 1–7.
- R. Turner et al., 2021. Bayesian optimization is superior to random search for machine learning hyperparameter tuning: analysis of the black-box optimization challenge 2020, In: *Proceedings of the NeurIPS 2020 Competition and Demonstration Track*, 2021: PMLR, pp. 3–26.
- Vaswani, A., et al., 2017. Attention is all you need. *Adv. Neural Inf. Process. Syst.* 30.
- Wang, Y., Li, J., Hao, H., 2022a. A state-of-the-art review of experimental and numerical studies on BLEVE overpressure prediction. *J. Loss Prev. Process Ind.* 80, 104920. <https://doi.org/10.1016/j.jlp.2022.104920>.
- Wang, Y., Li, J., Hao, H., 2022b. Development of efficient methods for prediction of medium to large scale BLEVE pressure in open space. *Process Saf. Environ. Prot.* 161, 421–435. <https://doi.org/10.1016/j.psep.2022.03.045>.